Available online at www.sciencedirect.com

ScienceDirect

Procedia Computer Science 200 (2022) 376–385

Procedia Computer Science

www.elsevier.com/locate/procedia

3rd International Conference on Industry 4.0 and Smart Manufacturing

Flexible robotic strategy for the assembly of ring-shaped elastic objects

Andrea Monguzzi, Marco Maiocchi, Andrea Maria Zanchettin, Paolo Rocco

Politecnico di Milano, DEIB, Piazza Leonardo da Vinci 32, 20133 Milano, Italy

Abstract

This paper addresses the challenge of the robotized insertion of ring-shaped elastic objects into parts' outer grooves, which is a key operation in several industrial processes. We propose a novel flexible strategy to insert ring-shaped elastic objects of different sizes and stiffnesses, exploiting a generic robot and a simple - yet effective - fixture. Despite the overall complexity of the procedure is entirely poured on the mentioned fixture, its simplicity of realization and implementation allows to equip the robot with a generic gripper, without the use of any additional sensor. The effectiveness of the proposed strategy is assessed via experimental tests, proving the efficiency and flexibility in the insertion of different ring-shaped elastic objects.

Keywords: Ring-shaped elastic object; robotics; flexible manufacturing; deformable object manipulation; assembly operation

1. Introduction

The fourth industrial revolution, or Industry 4.0, has introduced new technologies that are redefining the industrial production in smart factories. In particular, the introduction of collaborative robots (cobots) brought significant changes in the paradigm of industrial robotics, since the use of cobots can provide significant advantages, especially in terms of flexibility, as they can be employed in a variety of tasks, at a moderate installation cost.
The current industrial production is a competitive and continuously evolving framework, where flexibility and reconfigurability are essential: the ultimate objective is to assign to a single cobot the execution of different operations, avoiding any kind of interruption or discontinuity as, for example, setup times.

A recent study from McKinsey & Company [1] shows that more than 40% of occupations have at least 50% of their activities that are automatable. As a consequence, half of the operations of at least 40% of the jobs, where

E-mail address: andrea.monguzzi@polimi.it

1877-0509
10.1016/j.procs.2022.01.236

Fig. 1: Examples of the insertion of a ring-shaped elastic object into a outer part's groove.

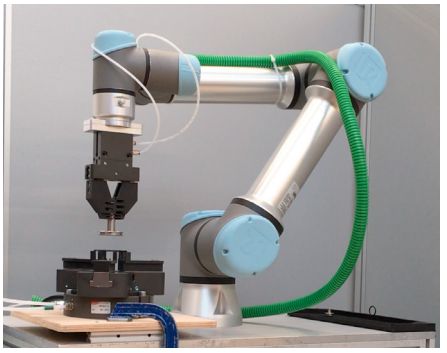

Fig. 2: Robotized insertion of o-rings.

assembly takes a large part, are automatable, while a consistent remainder of tasks can be, instead, carried out by human operators. In this paper, we focus on the manipulation of flexible and elastic objects, whose automatization is particularly challenging due to the required high dexterity.
To this regard, the insertion of ring-shaped elastic objects into the outer grooves of a part is a task often requested in the manufacturing industry and typically addressed either resorting to human intervention, with the aid of ad-hoc tools, or via heavy automation solutions. Nevertheless, such operation is fundamental in several industrial settings, such as automotive industry for the manufacture of engines, fuel systems, air conditioning, transmission to seal against oil, fuel, air, etc. Moreover it is also necessary in fields operating with food, beverage and drinking water, for example to insert seals in stoppers for jars and water bottles, or to assemble the containers of water filters. Furthermore ring-shaped elastic objects are used to produce cables connectors and quick couplings. Figure 1 shows some real applications of the insertion of a ring-shaped elastic object into a outer part's groove.

As a response to the request for flexibility, high production mix and large number of product variants that characterize the current manufacturing industry, this paper aims to present a solution to insert ring-shaped elastic objects, of different sizes and/or materials, into parts' outer grooves. Particularly, the method allows to realize a common insertion operation in a flexible way, exploiting an easily reprogrammable workstation. Moreover, the proposed strategy offers a cheaper solution than specialized machines for the insertion of ring-shaped elastic objects. The operation is indeed performed through an actuated fixture, easy to implement, whose actions are synchronized with these of the robot.

Sensors, ad-hoc grippers and specific kinds of robots are not required, as the only tasks the robot has to perform are the pick and place of the elastic objects and the manipulation of the rigid parts. Figure 2 shows the experimental setup of the proposed strategy for a selected use case presented in Section 5. In the light of the above, the proposed methodology lends itself to a straightforward use in a real industrial setup.

This paper is organized as follows. We present related works in Section 2 and provide details on the proposed strategy for the insertion of ring-shaped elastic objects into parts' outer grooves in Section 3, highlighting the differences with methods proposed in the literature. A routine is also presented to properly synchronize the actions between fixture and robot. Section 4 describes a method to select parameters for the design of fixture's fingertips, firstly focusing on their optimal design and then offering details for their production. Experimental validation of the proposed strategy applied to different o-rings and pistons' grooves is discussed in Section 5. Concluding remarks can be found in Section 6.

2. Related works

Robotic manipulation of deformable objects is a topic extensively studied in the literature since, as stated in [2], this ability is required in lots of different applications and could grant considerable economical benefits. However, the mentioned task requires high level of dexterity as explained in [3]: generally the manipulation of deformable

elements implies an under-constrained system. Deformable objects are, indeed, described by an infinite number of degrees of freedom, resulting in huge uncertainties during manipulation. In this framework, different studies have been carried out, especially concerning flexible linear objects, such as ropes, tubes and cables, analysing modelling strategies (from physical based models [4] to not physical ones[5],[6],[7]) together with a large number of applications, including cable routing and insertion [8], [9], [10], knotting operations [11], predicting and controlling the shape [12], and finally suppressing vibration [13]. However, there have been few works dealing with ring-shaped flexible objects, that are the main focus of the present work.

Particularly, [14] presents a method to plan the motion of a flexible object, based on simulation using Finite Element Method, that is then applied to ring-shape elastic objects subject to large deformation, manipulated by dual arm robots. The result can be exploited to plan the trajectory for robotic hands to perform the considered operation.

The assembly of a rubber belt on fixed pulleys is instead discussed in [15]: the belt is first inserted into a small pulley and then is stretched to allow its insertion into a larger one.

Motion planning for a dual arm cobot to perform the assembly of ring-shaped elastic objects is investigated in [16] and [17]. They propose the combination of an assembly task planner, that computes the key configurations of the robot's end effectors, with an optimization-based assembly step planner, defining the motion between the configurations. The main goal pursued is the minimization of the elastic object's deformation during the execution of the procedure. However, as reported in [16], the presented method is suitable mainly for elastic object with moderate stiffness. [18], building on [17], discusses a strategy to generate the key positions, used as partial goals in the motion planning algorithm, exploiting captured human movements during the execution of the operation.

A force control method, based on human data, to insert a ring shaped elastic part is presented in [19]. Here the elastic part is held in position against the groove thanks to a rotating fixture. In the meanwhile, the robot, equipped with an ad-hoc tool, composed of a thin rod-shaped and a force sensor, performs the operation, trying to minimize the force acting on the elastic part.

[20] states that, in the industrial framework, the considered operation is usually carried out manually by human operators, sometimes with the aid of ad-hoc tools, or thanks to specialized machines in case of high volume production. Moreover some specialized and complex grippers for robots, as, for example, the ORG gripper by Schunk, can be mounted on the robot to automatize the operation under study, as shown in [20].

3. Problem statement and contributions

The task faced in this paper deals with the insertion of ring-shaped elastic objects into parts' outer grooves: usually each elastic object is paired with the corresponding part where it has to be inserted. The framework can be generalized considering all the tuples $(r_{ci}, r_{ni}, h_i), i \in \{1, ..., I\} = \mathcal{R}$ where r_{ci} refers to the inner radius of the ring-shaped elastic object, while r_{ni} and h_i are, respectively, the nominal external radius and the insertion height (given by the length between the beginning of the groove and the extreme edge) of the corresponding part where the elastic object has to be inserted. Finally, $\mathcal{R}$ represents the set of paired objects. The goal is hence to design a fixture and create a routine to insert elastic objects of radii r_{ci} on the related parts of radii r_{ni}. Figure 3 shows three different elastics rings and the corresponding pistons.

As mentioned in Section 1, the fixture should be simple to implement: indeed it consists of a double effect pneumatic gripper as the one shown on the left in Figure 2, equipped with three jaws, custom fingertips and a pair of electronic proportional regulators to control the amount of pressure supplied to the gripper to open and close jaws. In particular, each jaw is equipped with a custom fingertip characterized by a stair configuration, as the one shown in Figure 4. Section 4 deals with the optimal design of fingertips given a set $\mathcal{R}$ and specification on the gripper's stroke.

Together with the design of the fixture, we propose a sequence of operations to perform the insertion. The fingertips allow to enlarge in a hexagonal shape the elastic object, previously placed on the pins (Figure 4) without stretching it. By controlling the opening and the closing of jaws, thanks to the pair of electronic proportional regulators, it is possible to enlarge the elastic object of radius r_{ci} in a configuration that lets the robot insert from above the part with radius r_{ni} without any contact, bringing the grove at the same height of the elastic object. At this point the jaws close on the component without pressing against it, allowing the elastic object to partially enter the part's groove. Finally,

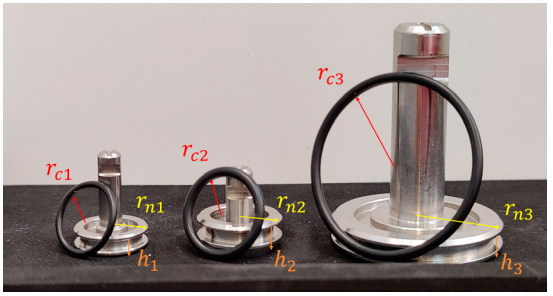

Fig. 3: Pairs of different o-rings and pistons. Dimensions $(r_{ci}, r_{ni}, h_i), i = 1, ..., 3$ are highlighted.

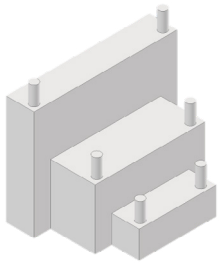

Fig. 4: Model of a custom fingertip.

the robot lifts the part: the elastic object, partially trapped in the groove, follows it, completing the insertion and avoiding possible twists of the ring-shaped object that would lead to an unsatisfactory result.

Comparing the proposed solution to the methods presented in Section 2, it can be pointed out that it does not require a specific robot, while a dual arm is necessary in [16], [17] and [18], and no additional sensors are needed, in contrast to the approach presented in [19]. Large elastic expansion, necessary in the manipulation executed by a dual arm, as explained in [14], are also avoided.
Furthermore previous strategies do not deal with the grasping phase of the elastic object, directly positioned in the ad-hoc grippers ([16], [17], [18]) or in the fixture ([19]). On the contrary, in the presented strategy, the robot is equipped with a generic parallel gripper. This enables the grasping of the elastic components and of the parts, creating a flexible framework that can be exploited also to perform other operations, without the need of a change of setup, in contrast to what proposed in [20]. The use of ad-hoc grippers can also bring to problems related to the stiffness of the different elastic objects considered, as mentioned for example in [16], where the designed holder for grasping the ring-shaped object got detached, from the robot's finger, due to its high stiffness. On the other hand, methods as the one explained in [19] are suitable especially for stiff elastic objects.
Summing up, our method suggests a flexible solution to insert different kinds of ring-shaped elastic objects with various sizes and stiffnesses, using conventional and general purpose hardware.

4. Design of the fingertips

This Section deals with the design of custom fingertips to perform the insertion operation for a given set of tuples $(r_{ci}, r_{ni}, h_i), i \in \{1, ..., I\} = \mathcal{R}$, ordered from the smallest to the largest r_{ci}. As Figure 4 shows, fingertips are designed according to a stair configuration, composed by different steps: a single step can be exploited to execute the considered operation on different tuples (r_{ci}, r_{ni}, h_i) and multiple steps are needed to perform all the required insertions.
It is quite evident that the design of the fingertips can be split in two phases:

- Selection of the parameters to design a single step, starting from a given tuple (r_{ci}, r_{ni}, h_i), aiming to place the elastic object with inner radius r_{ci} on the fixture without deforming it and to insert the highest number of subsequent pairs.
- Introduction of the physical realization constraints and computation of the needed number of steps.

4.1. Selection of the parameters for the creation of a step

Each step is composed by a horizontal plate where two vertical pins are inserted. The design of steps must start from the tuple (r_{c1}, r_{n1}, h_1), characterized by the smallest r_{ci}, to prevent plates from colliding when jaws close.
A single step is identified by a certain height, defined according to the values h_i of the parts where elastic objects have to be inserted, and by a plate of dimensions a, b as shown in Figure 5. Pins are characterized by a radius r_s that,

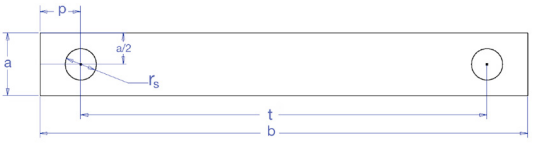

Fig. 5: Top view of the plate of a fingertip's step.

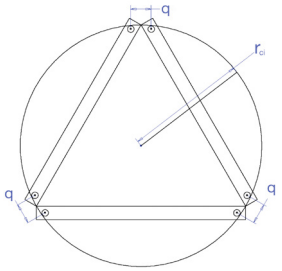

Fig. 6: Top view of plates of the three fingertips and elastic object of radius r_{ci}.

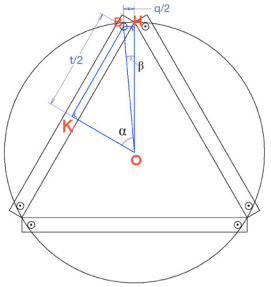

Fig. 7: Relationship between q and t.

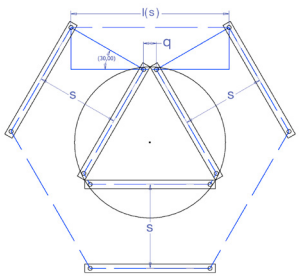

Fig. 8: Definition of $l(s)$.

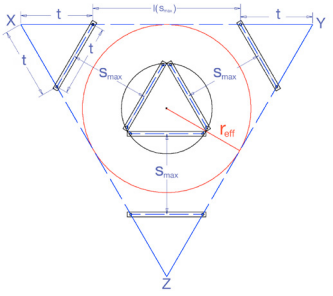

Fig. 9: Equilateral triangle obtained.

as tests highlighted, is an important design parameter, since it has a strong influence in the final part of the operations when jaws close: the smaller r_s is, the more jaws can be closed without entering in contact with the part, allowing the ring-shape object to enter the groove. It follows that r_s should be as small as possible, however construction limits arise due to the type of the material used and to the stiffness of the elastic object: it is indeed fundamental that pins do not deform during the execution of the operation.

Figure 6 shows a top view of three plates, corresponding to three fingertips mounted on the jaws. As we want to insert the elastic object of radius r_{c1} without deforming it when jaws are closed, the situation should be similar to the one described in Figure 6. Since the design starts considering the elastic object with the smallest radius, pins must be designed as close as possible to the corresponding circumference, as Figure 6 shows.

It is then necessary to determine the parameters t and q to obtain such a configuration. The lengths a and p have to be chosen according to the design of the fingertips and the constructive limits given by the material used, i.e. $a \geq a_{min}$ and $p \geq p_{min}$.

It is also possible to explicitly link the design parameters t and q. In this phase we can assume in fact that $r_s \ll r_{ci}$, meaning that $r_{ci} - r_s \approx r_{ci}$. Considering Figure 7, and, particularly, the right triangles BKO and BHO, it holds that $t = 2r_{ci}\sin(\alpha)$ and $q = 2r_{ci}\sin(\beta)$. Since it holds $\alpha + \beta = 60°$ and due to the fact $\beta = \beta(q)$, in particular $cos(\beta) = (\sqrt{4r_{ci}^2 - q^2})/2r_{ci}$, we can finally write:

$$t = \frac{\sqrt{3}}{2}\sqrt{4r_{ci}^2 - q^2} - \frac{q}{2} \tag{1}$$

Equation 1 shows that if q increases, t decreases and vice-versa. Moreover, taking into account the condition of existence of the root and imposing $t > 0$ and $q > 0$ we obtain, respectively, $0 < q < 2r_{ci}$ and $0 < q < \sqrt{3}r_{ci}$.

In the following, q is considered as an independent variable: once its optimal value is determined, it will be possible to compute the value of t exploiting 1.

The parameter q takes values in a closed interval: the upper bound is given by the value of q such that $t = 0$, while the lower bound can be found geometrically considering Figures 5 and 6. We can conclude that $q \in (\delta, \sqrt{3}r_{ci})$, where $\delta = p + \sqrt{3}a/2$.

Moreover, defining the stroke covered by the jaws as s, with $0 \leq s \leq s_{max}$, it holds that $l(s) = q + 2s \cdot cos(30°)$, as it is evident from Figure 8.

The goal is to enlarge the elastic object in a configuration that brings to the identification of the circumference of maximum effective radius r_{eff}. This circumference is inscribed in the equilateral triangle XYZ, obtained by extending

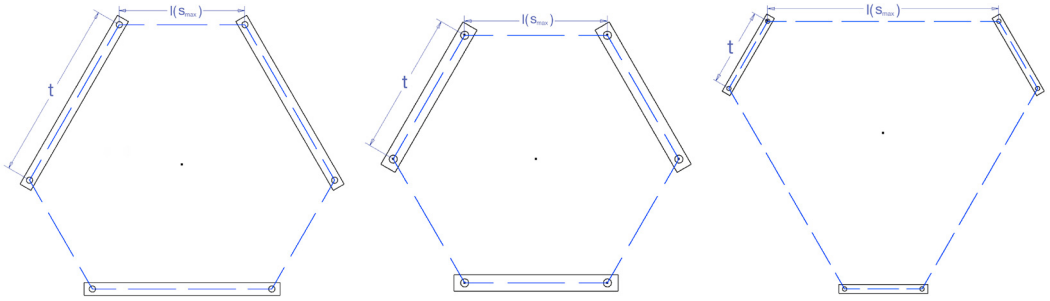

(a) (b) (c)

Fig. 10: Different configurations obtained depending on the relationship between t and $l(s_{max})$: $t > l(s_{max})$ (a), $t = l(s_{max})$ (b), $t < l(s_{max})$ (c).

the biggest sides of the irregular hexagon created enlarging the elastic object, exploiting all the available stroke of the chosen pneumatic gripper, s_{max}. Figure 9 shows an example of the cited equilateral triangle together with the circumference of radius r_{eff}. As shown in Figure 10, the biggest side of the mentioned irregular hexagon is determined by the relationship between t and $l(s_{max})$, leading to three different cases. It follows that a particular choice of q strongly influences the way in which the elastic object is deformed when jaws open.

Considering the configuration case in which $l(s_{max}) = t$, i.e. case (b) in Figure 10, it is possible to compute the value of q as follows:

$$q = \gamma = -\frac{\sqrt{3}s_{max}}{2} + \frac{\sqrt{4r_{ci}^2 - s_{max}^2}}{2} \tag{2}$$

If $r_{ci} \geq s_{max}/2$, this relation is always well defined.

However, recalling that $q \in (\delta,\ \sqrt{3}r_{ci})$, it follows that $\gamma \in (\delta,\ \sqrt{3}r_{ci})$ implying $r_{ci} \geq \sqrt{\delta^2 + s_{max}^2 + \sqrt{3}\delta s_{max}}$.

Therefore, if the previous constrain is satisfied, all the three configuration cases of Figure 10 can be obtained: case (a) if $q < \gamma$, case (b) if $q = \gamma$ and case (c) if $q > \gamma$. On the other hand, if $\gamma < \delta$, only the configuration reported in case(c) is feasible, since q must be greater than δ. Therefore, it is possible to conclude that the configuration obtained in the case $s = s_{max}$, as well as those obtained in the transitional phase, strictly depend on the relationship between q and γ, which in turn depend on geometric constraints.

Recalling that the goal is to create a step able to enlarge the highest number of tuples (r_{ci}, r_{ni}, h_i), the value $q^* = argmax(r_{eff})$ must be determined. Considering the three configurations reported in Figure 10, the expressions of the effective radius r_{eff} can be listed as follows:

$$r_{eff} = \begin{cases} \frac{\sqrt{3}}{6}(2\sqrt{3}s_{max} + \frac{3}{2}q + \frac{\sqrt{3}}{2}\sqrt{4r_{ci}^2 - q^2}), & case(a) \\ \frac{3}{4}\sqrt{4r_{ci}^2 - q^2} - \frac{3}{4\sqrt{3}}q, & case(b) \\ \frac{s_{max}}{2} + \frac{\sqrt{4r_{ci}^2 - q^2}}{2}, & case(c) \end{cases} \tag{3}$$

Computing and studying the derivative $\partial r_{eff}/\partial q$, it can be seen that r_{eff} is maximum if q takes the maximum value in case (a) and the smallest possible value in cases (b) and (c). Recalling the results obtained imposing the other obtained conditions, we can conclude that:

$$r_{eff}|_{max} \text{ for } \begin{cases} q^* = \gamma, & \text{if } r_{ci} \geq \sqrt{\delta^2 + s_{max}^2 + \sqrt{3}\delta s_{max}} \\ q^* = \delta, & \text{if } r_{ci} < \sqrt{\delta^2 + s_{max}^2 + \sqrt{3}\delta s_{max}} \end{cases} \tag{4}$$

Once q is determined, t can be computed according to Equation (1) and the other parameters have to be designed according to the observations contained in the following.

4.2. Realization constraints and computation of the needed number of steps

In the previous Subsection all the assumptions are valid from geometrical and theoretical point of view. However, the manufacturing of fingertips must take into account elements such as the radius of pins, design tolerances and constructive limits given by the chosen material. Defining $\delta_{r_{ci}} = r_{ci} - r_s$, $\Delta_{r_{ci}}$ and $\Delta_{r_{ni}}$, respectively, as the values of the tolerances that allow the insertion without contact of the ring-shaped object and the corresponding part with the fingertips, Algorithm 1 provides the pseudo-code to identify the number of required steps d. Each iteration $j = 1, ..., d$ of the algorithm corresponds to the creation of one step for the fingertips.

Algorithm 1 fingertips design

Input: All the tuples $(r_{ci}, r_{ni}, h_i), i \in \{1, ..., I\} = \mathcal{R}$ ordered in ascending order, according to the value of r_{ci}

1: $j = 1$
2: $k^* = 1$
3: $\delta r_c|_{minj} = \delta r_{c1} - \Delta r_{c1}$
4: **repeat**
5: Define a_j, p_j according to physical constraints $a_{j_{min}}$ and $p_{j_{min}}$
6: **if** $\delta r_c|_{minj} < \sqrt{\delta^2 + s_{max}^2 + \sqrt{3}\delta s_{max}}$ **then**
7: Determine q_j starting from $\delta r_c|_{minj}$
8: Compute t_j
9: **if** $0 \le t_j \le 2r_s$ **then**
10: Set $t_j = 0$, recompute q_j and compute $r_{eff}|_{maxj}$
11: **else if** $t_j > 2r_s$ **then**
12: Compute $r_{eff}|_{maxj}$
13: **end if**
14: **else if** $\delta r_c|_{minj} \ge \sqrt{\delta^2 + s_{max}^2 + \sqrt{3}\delta s_{max}}$ **then**
15: Determine q_j starting from $\delta r_c|_{minj}$
16: Compute t_j and $r_{eff}|_{maxj}$
17: **end if**
18: **if** $r_{eff}|_{maxj} \ge r_{nI} + \Delta r_{nI} - r_s$ **then**
19: $r_n|_{maxj} = r_{nI}$
20: $k^* = \arg \max_{k \in \mathbb{Z}: k = k^* ... I} \{h_k\}$
21: $h_{maxj} = h_{k^*}$
22: **else if** $r_{eff}|_{maxj} < r_{nI} + \Delta r_{nI} - r_s$ **then**
23: $i^* = \arg \min_{i \in \mathcal{R}: r_{ni} + \Delta r_{ni} > r_{eff}|_{maxj} + r_s} \{r_{ni}\}$
24: $r_n|_{maxj} = r_{n(i^*-1)}$
25: $k^* = \arg \max_{k \in \mathbb{Z}: k = k^* ... i^*-1} \{h_k\}$
26: $h_{maxj} = h_{k^*}$
27: $k^* = i^*$
28: $j = j + 1$
29: $\delta r_c|_{minj} = \delta r_{ci^*} - \Delta r_{ci^*}$
30: **end if**
31: **until** $r_n|_{maxj} = r_{nI}$

Output: $d = j$, design parameters

The procedure starts initializing $j = 1$ (first iteration) and considering the elastic object with the smallest radius setting $\delta r_c|_{minj} = r_{c1} - r_{s1}$: a step is built to maximize $r_{eff}|_{maxj}$. The designed step allows to execute the insertion operation for all the tuples (r_{ci}, r_{ni}, h_i) that have $r_{ci} - r_s - \Delta r_{ci} \ge r_c|_{minj}$, $r_{ni} + \Delta r_{ni} \le r_n|_{maxj} + r_s$ and $h_i \le h_{maxj}$ (where $r_n|_{maxj}$ is computed as $r_{n(i^*-1)}$ and i^* is the subscript corresponding to the minimum r_{ni} bigger than $r_{eff}|_{maxj} + r_s - \Delta r_{ni}$). If $r_n|_{maxj} = r_{nI}$, it follows that all the tuples in $\mathcal{R}$ can be inserted, otherwise an additional step must be designed: j is increased and the procedure is repeated considering $\delta r_c|_{minj} = \delta r_{ci^*} - \Delta r_{ci^*}$. It should be noticed that the elastic objects with radius $r_{ci} < r_{min} + \Delta r_{ci}$, where $r_{min} = a_{min}/2 + p_{min}/\sqrt{3}$, must not be considered due to physical realization constraints.

In some cases, especially for small elastic object radii, it may happen that the algorithm generates an overlap of the pins configuration resulting in an unfeasible solution. Therefore, in these cases the problem can be solved by adopting a triangular configuration, i.e. the two pins of the fingertips are substituted by a single pin. The described situation is checked in lines 9-10 of Algorithm 1.

Notice that the height value h_{maxj} represents the minimum height of the step j with respect to the step $j - 1$ that must be taken into account in order to allow the correct insertion of the ring-shaped elastic objects into part's outer grooves. Different solutions can be adopted, but the most suitable one is the one reported in Figure 11 where the height of the pins is slightly greater than the thickness of the elastic object. In fact, the reported fingertips design has mainly two advantages: the first one is the minimization of the bending of the pin during the enlargement phase, while the second one is related to the positioning repeatability of the elastic object. The proposed fingertips design requires the pins to be on the edge of the step, otherwise the base of the fingertips would come into contact with the part that has to

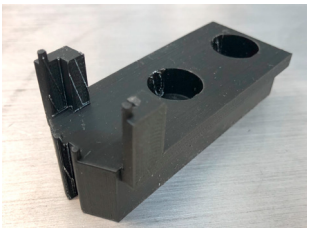

Fig. 11: Custom fingertip for the fixture.

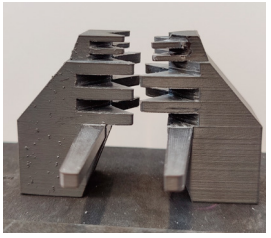

Fig. 12: Custom fingertip for the UR5 gripper.

be inserted. Finally, it should be noticed that it is assumed that the part's outer groove always makes contact with the elastic object before it touches the pins, otherwise the insertion operation is not feasible. Therefore, the value of the pins' radius must be appropriately determined according to both the reported consideration and, as already mentioned, the physical realization constraints.

5. Experimental results: insertion of an o-ring into a piston's groove

In this Section the effectiveness of the proposed strategy is experimentally validated on a case study: the insertion of an o-ring on a piston's groove, a situation that is very common in the assembly of pneumatic systems. Particularly, three HNBR o-rings (Young's modulus of 6.6 MPa) are considered, with the corresponding pistons. The dimensions of these objects, shown in Figure 3, are summarized in the first three rows of Table 1.

Table 1: O-rings and pistons dimensions and chosen parameters used as input of Algorithm 1.

	$i = 1$	$i = 2$	$i = 3$
$r_{ci}[mm]$	7.80	8.57	19.67
$r_{ni}[mm]$	9.42	10.95	21.95
$h_i[mm]$	3.80	4.90	5.50
$\Delta r_{ci}[mm]$	0.5	0.5	0.5
$\Delta r_{ni}[mm]$	0.5	0.5	0.5
$r_s[mm]$	1	1	1
$a_{min}[mm]$	1	1	1
$p_{min}[mm]$	5.33	5.33	5.33

The fixture's fingertips are designed according to Algorithm 1: the last five rows of Table 1 summarize the values used for the input parameters. The result are three fingertips, characterized by two different steps to insert the three different o-rings. Figure 11 depicts one of the fingertips, build in 3D printing.

5.1. Workbench setup

The experimental setup is shown in Figure 2: a support to hold o-rings and pistons is visible on the right, followed by the cobot, in the middle, and finally by the proposed fixture configuration. The robot used in this paper for experimental validation is a UR5 by Universal Robots. This collaborative robot is in fact suitable for the insertion of the o-rings, having a sufficient payload and not requiring the presence of protective barriers, increasing the reconfigurability of the workstation. Moreover, safety for human-robot cooperation could be ensured by simple measures, such as the use of an electric gripper, mounted on the cobot, and a protective box around the proposed fixture or a proximity sensor that allows to block it in case of emergency. The UR5 is customized with a Camozzi's pneumatic parallel gripper and custom 3D printed fingertips. Figure 12 shows the particular design chosen for the fingertips, which allows to grasp different o-ring sizes and a wider range of parts with respect to a round C shape design, allowing to have more than only two contact points.

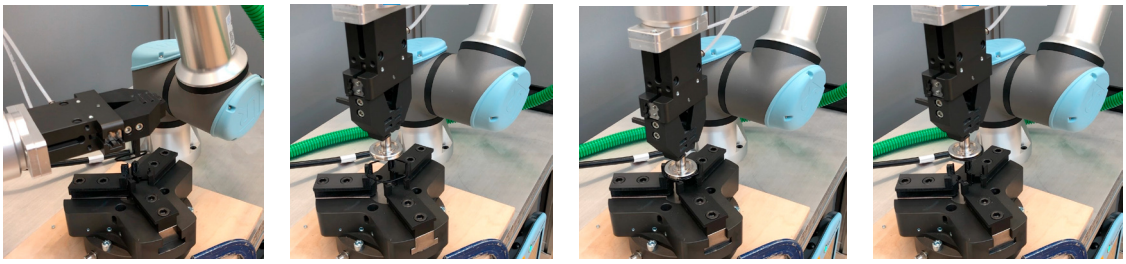

(a) (b) (c) (d)

Fig. 13: Snapshots taken from one of the experiments of o-ring insertion in the piston's groove.

To make the fixture, a CGZT gripper of bore 160 by Camozzi, characterized by an available stoke of 16.0 *mm*, is selected. The CGZT is a double effect, pneumatic gripper with three jaws. A pair of electronic proportional micro regulators of series K8P by Camozzi are used to control the amount of pressure supplied to the gripper to open and close jaws. Solenoid valves and K8P regulators, pneumatically connected to one of them, are plugged into the control box of the UR5. It is important to stress that there is a linear relationship between the value of the analogue input and the downstream pressure of the proportional regulator. Moreover, the relation among the time, in which the analogue input of K8Ps is kept high, and the obtained value of the CGZT stroke is also linear regardless the supplied pressure to K8Ps. It follows that it possible to compute the time necessary to enlarge the o-ring in order to allow the correct insertion of the piston from above.

5.2. Experimental results

The task consists in performing the insertion of the two o-rings characterized by r_{c2} and r_{c3} in the corresponding pistons' groove. Firstly, in both cases, the UR5 approaches and grasps the o-ring and brings it to the fixture to deposit it (Figure 13a). After that, the o-ring is enlarged until it reaches a configuration that allows to insert the piston from above, as shown in Figure 13b. The cobot inserts the piston and, once its groove is at the same height of the o-ring, CGZT's jaws begin to close, arriving to a predefined configuration (Figure 13c). Finally, the UR5 lifts the piston and the o-ring follows it, being trapped in its groove: the operation ends correctly as shown in Figure 13d. It is important to highlight that the times in which the jaws open and close are computed depending on the required o-ring deformation.

The accompanying video (https://www.youtube.com/watch?v=lxhoX34mooo) shows a complete execution of both operations. In order to analyse the effectiveness of the proposed strategy, the insertions have been repeated several times with a success rate of about 95%, replacing the o-ring at each test and performing the operation successfully, despite the ring-shaped object is positioned by hand on the support. The o-rings' diameter affects the success rate, since initial positioning uncertainties are more relevant for correct placement and enlargement of smaller o-rings. In an industrial implementation of the proposed strategy, an automatic feeder can be then exploited to reduce the uncertainty in the elastic object's position. The execution time is acceptable, being around 30 *s* for each complete iteration. Moreover it is also similar to the time required to manually perform the operation with the aid of a tool.

6. Conclusion

This paper deals with the challenging task of the insertion of ring-shaped elastic objects into part's outer grooves. Particularly, the task addressed is the insertion of ring-shaped elastic objects characterized by different size and stiffness without the need of setup times.
Compared to methods proposed in the literature, the presented strategy focuses on the creation of a solution that does not require a specific kind of robot and allows to execute also other tasks, avoiding the use of had-hoc grippers and meeting the requirement of flexibility that is becoming essential in the current industrial production. The presented

fixture is simple to produce and implement and it does not require any sensors, as it is setup with a pneumatic double effect gripper with three jaws, two proportional regulators, to control the amount of pressure supplied to the gripper, and custom fingertips. In this regard, we propose a method to properly select the parameters to design the fingertips in a stair configuration, considering the stroke of the three jaws gripper, allowing to insert all the considered elastic objects on the corresponding parts, according to the presented strategy. Together with a study on the optimal design of the fingertips, a detailed analysis about their physical realization is carried out.
The proposed approach has been experimentally validated on the insertion of two o-rings on related pistons' groove, 3D printing the fingertips and using the UR5 by Universal Robots.
In the future, we would like to improve robustness against a considerable number of industrial cycles considering a more suitable material to produce the fingertips. In addition, a high number of ring-shaped objects should be considered, in order to obtain a considerable number of steps to practically test the efficiency of the proposed strategy.

Acknowledgements

The authors would like to thank Camozzi Automation, part of a Joint Research Centre together with Politecnico of Milan, for providing the material and the know-how about the instrumentation.

References

[1] McKinsey & Company, "A future that works: automation, employement, and productivity", available at https://www.mckinsey.com/~/media/mckinsey/featured%20insights/Digital%20Disruption/Harnessing%20automation%20for%20a%20future%20that%20works/MGI-A-future-that-works-Executive-summary.ashx.
[2] Sanchez, J., Corrales, J. A., Bouzgarrou, B. C., and Mezouar, Y. (2018). "Robotic manipulation and sensing of deformable objects in domestic and industrial applications: a survey."*The International Journal of Robotics Research*, **37(7)**, 688-716.
[3] Chatzilygeroudis, K., Fichera, B., Lauzana, I., Bu, F., Yao, K., Khadivar, F., and Billard, A. (2020). "Benchmark for bimanual robotic manipulation of semi-deformable objects." *IEEE Robotics and Automation Letters*,**5(2)**, 2443-2450.
[4] Lv, N., Liu, J., Xia, H., Ma, J., and Yang, X. (2020). "A review of techniques for modeling flexible cables." *Computer-Aided Design*, 122, 102826.
[5] Palli, G. (2020, June). "Model-based Manipulation of Deformable Linear Objects by Multivariate Dynamic Splines." *In 2020 IEEE Conference on Industrial Cyberphysical Systems (ICPS)*, Vol. 1, 520-525.
[6] Maffezzoni, C., and Rocco, P. (2001). "The index of PDAEs applied to the modelling of a flexible mechanical system." *Mathematical and Computer Modelling of Dynamical Systems*, **7(3)**, 305-321.
[7] Navarro-Alarcon, D., and Liu, Y. H. (2017). "Fourier-based shape servoing: a new feedback method to actively deform soft objects into desired 2-D image contours." *IEEE Transactions on Robotics*, **34(1)**, 272-279.
[8] Zheng, Y. F., Pei, R., and Chen, C. (1991). "Strategies for automatic assembly of deformable objects. In Proceedings." *1991 IEEE International Conference on Robotics and Automation*, 2598-2599.
[9] Nakagaki, H., Kitagaki, K., Ogasawara, T., and Tsukune, H. (1997). "Study of deformation and insertion tasks of a flexible wire." *In Proceedings of International Conference on Robotics and Automation*, Vol. 3, 2397-2402. IEEE.
[10] Palli, G., and Pirozzi, S. (2019). "A tactile-based wire manipulation system for manufacturing applications." *Robotics*, **8(2)**, 46.
[11] Saha, M., and Isto, P. (2007). "Manipulation planning for deformable linear objects." *IEEE Transactions on Robotics*, **23(6)**, 1141-1150.
[12] Zhu, J., Navarro, B., Fraisse, P., Crosnier, A., and Cherubini, A. (2018). "Dual-arm robotic manipulation of flexible cables." *2018 IEEE/RSJ International Conference on Intelligent Robots and Systems (IROS)*, 479-484.
[13] Ding, F., Huang, J., Matsuno, T., and Fukuda, T. (2011). "Skill-based vibration suppression in manipulation of deformable linear objects." *2011 International Symposium on Micro-NanoMechatronics and Human Science*, 421-426).
[14] Yoshida, E., Ayusawa, K., Ramirez-Alpizar, I. G., Harada, K., Duriez, C., and Kheddar, A. (2015). "Simulation-based optimal motion planning for deformable object." *2015 IEEE international workshop on advanced robotics and its social impacts (ARSO)*, 1-6.
[15] Miura, J., and Ikeuchi, K. (1998). "Task planning of assembly of flexible objects and vision-based verification." *Robotica*, **16(3)**, 297-307.
[16] Ramirez-Alpizar, I. G., Harada, K., and Yoshida, E. (2018). "A simple assembly planner for the insertion of ring-shaped deformable objects." *Assembly Automation*.
[17] Ramirez-Alpizar, I. G., Harada, K., and Yoshida, E. (2014). "Motion planning for dual-arm assembly of ring-shaped elastic objects." *2014 IEEE-RAS International Conference on Humanoid Robots*, 594-600.
[18] Ramirez-Alpizar, I. G., Harada, K., and Yoshida, E. (2017). "Human-based framework for the assembly of elastic objects by a dual-arm robot." *Robomech Journal*, **4(1)**, 1-10.
[19] Fukumoto, Y., and Harada, K. (2018). "Force Control Law Selection for Elastic Part Assembly from Human Data and Parameter Optimization." *2018 IEEE-RAS 18th International Conference on Humanoid Robots (Humanoids)*, 1-7. IEEE.
[20] Fast-Berglund, Å., Palmkvist, F., Nyqvist, P., Ekered, S., and Åkerman, M. (2016). "Evaluating cobots for final assembly". *Procedia CIRP*, **44**, 175-180.